




Magnetic Bloch-point hopping in multilayer skyrmions and associated emergent electromagnetic signatures

Yu Li (李昱)^{1,*}, Sergiy Mankovsky², Svitlana Polesya,² Hubert Ebert² and Christoforos Moutafis^{1,†}

¹*Nano Engineering and Spintronic Technologies (NEST) Group, Department of Computer Science, University of Manchester, Manchester M13 9PL, United Kingdom*

²*Department Chemie/Physikalische Chemie, Ludwig-Maximilians-Universität München, Butenandtstrasse 5-13, 81377 München, Germany*



(Received 2 July 2021; revised 28 September 2021; accepted 4 October 2021; published 27 October 2021; corrected 3 December 2021)

Magnetic multilayers are promising tunable systems for hosting magnetic skyrmions at/above room temperature. Revealing their intriguing switching mechanisms and associated inherent electrical responses are prerequisites for developing skyrmionic devices. In this Letter, we theoretically demonstrate the annihilation of single skyrmions occurring through a multilayer structure, which is mediated by the hopping dynamics of topological hedgehog singularities known as Bloch points. The emerging intralayer dynamics of Bloch points are dominated by the Dzyaloshinskii-Moriya interaction, and their propagation can give rise to solenoidal emergent electric fields in the vicinity. Moreover, as the topology of spin textures can dominate their emergent magnetic properties, we show that the Bloch-point hopping through the multilayer will modulate the associated topological Hall response, with the magnitude proportional to the effective topological charge. We also investigate the thermodynamic stability of these states regarding the layer-dependent magnetic properties. This study casts light on the emergent electromagnetic signatures of skyrmion-based spintronics, rooted in magnetic-multilayer systems.

DOI: [10.1103/PhysRevB.104.L140409](https://doi.org/10.1103/PhysRevB.104.L140409)

Introduction. Magnetic skyrmions are nontrivial spin textures (Fig. 1) that have remarkable stability due to their unique topological properties in nature, and have been proposed as candidates of information carriers especially following the recent demonstrations of individual skyrmions in magnetic materials [1–3]. The skyrmion stabilization highly relies on the competition between the isotropic Heisenberg exchange and antisymmetric Dzyaloshinskii-Moriya interaction (DMI) [4,5], accompanied by a magnetostatic interaction [6–9]. Various types of skyrmionic textures have been proposed concerning the class of DMIs arising from different crystal families. Their nontrivial topology can be characterized by the topological charge [2,10]

$$Q = \frac{1}{4\pi} \int \mathbf{s} \cdot (\partial_x \mathbf{s} \times \partial_y \mathbf{s}) dx dy. \quad (1)$$

Importantly, magnetic thin films stacked in nonmagnetic/ferromagnetic (NM/FM) multilayers give rise to a strong spin-orbit coupling, which in combination with the broken symmetry at the interfaces can result in a large additive DMI magnitude [11–13]. This can enable an excellent tunability in such material systems by precisely engineering the layer properties, making it therefore possible to stabilize magnetic skyrmions even at room temperature [13–15].

The topological constraints of magnetic skyrmions can be broken by the emergence of point singularities in magnets,

known as Bloch points [16] [Fig. 1(c)]. They are extremely small topological defects with magnetization vanishing in the core, where the continuum micromagnetic approach breaks down. It has been shown that the Bloch points play crucial roles in mediating the winding/unwinding processes of magnetic skyrmions, and their propagation has been thus far proposed in bulk chiral magnets [9,17,18] and magnetic multilayers [19]. Notably, the discontinuity in the multilayer structures due to the separation of ferromagnetic sites by nonmagnetic spacers, results in much more complex Bloch-point dynamics during the skyrmion unwinding process. Moreover, the interplay between Bloch points with magnetic skyrmions in three-dimensional multilayers, as well as the associated exotic emergent-field considerations, are particularly intriguing and largely missing.

As one skyrmion holds quantized “emergent flux” upon integration over a unit sphere S^2 [2,20–22], conduction electrons passing through the topologically nontrivial texture will be deflected into the direction transverse to the current flow, causing a topological Hall (TH) effect [23–30]. This type of Hall contribution is invariant and robust against continuous deformation: The strength of the TH signal, such as TH resistivity ρ_{xy}^{TH} , is independent of the domain size but purely determined by the topology of skyrmionic textures. Therefore, the TH response is able to act as an indicator for the presence of skyrmions, which has been experimentally evidenced in various types of materials, including bulk chiral magnets [25,26] and magnetic multilayers [29,30]. It enables a way to read out the skyrmion state by simply measuring the electronic transport response, which has technological relevances for possible future applications of

*YuLi.nano@outlook.com

†Christoforos.Moutafis@manchester.ac.uk

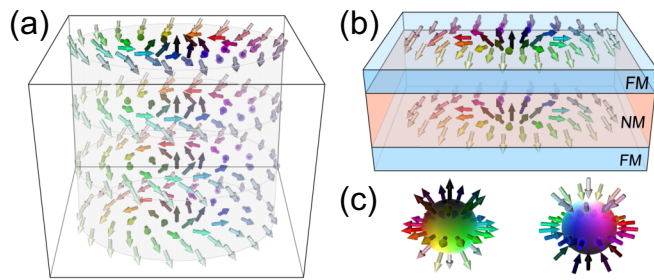


FIG. 1. Topologically nontrivial spin textures in ferromagnets. (a) Bloch-type skyrmion tube in bulk chiral magnets (such as FeGe). (b) Néel-type skyrmion “chain” in magnetic multilayers, with spin configurations only situated in the FM layers. (c) Bloch-point singularities with positive (left) and negative (right) topological charges, referred to as BP^+ and BP^- , respectively.

skyrmion-based spintronic devices. However, studies so far only focus on the electrical signature of skyrmionic textures in quasi-two-dimensional systems. Deeper understandings of the signature of skyrmionic textures in magnetic multilayers must necessarily consider (i) the coupling of skyrmions through layers [30,31], (ii) the depth-resolved dynamics of complex spin textures [9,32], and (iii) the correlation between the underlying variation of the TH signal and Bloch-point dynamics especially when the integrity of single skyrmions is broken [33], in which case more fundamental studies are essential.

In this Letter, we start from the chiral magnetization profile of a single skyrmion in a [Pt/Co/Ta]₂ multilayer and identify the complex annihilation dynamics mediated by Bloch points, involving their intralayer propagations and interlayer

Bloch-point hopping processes. The Bloch-point propagation within a Co layer has an oscillatory velocity and could give rise to an emergent electric field. The resulting hopping of Bloch points induces a variation of the TH signal, such as its manifestation in the TH resistivity ρ_{xy}^{TH} . We subsequently propose that the intermediate states during Bloch-point hoppings can be stabilized by engineering material properties in a layer-dependent manner, and these states can be well defined by TH properties. Our work then suggests a simple but efficient concept of multistate skyrmionic devices by fully utilizing the emergent electromagnetic signatures embedded in three-dimensional magnetic multilayers.

Bloch-point dynamics in multilayer. In the multilayer regime, when the thickness of individual FM layers is hitting the limit of micromagnetics, any finer meshes down to subnanometers become unrealistic [34]. Therefore, we perform the spin dynamics simulations in an atomistic scheme, using the open-source SPIRIT code [34]. Here, we consider a [Pt (1 nm)/Co/Ta (1 nm)]₂ system, including 100 cell \times 100 cell \times 5 cell in each Co layer with periodic boundary conditions applied in the xy plane. The pairwise isotropic exchange interactions J_{ij} [Fig. 2(h)] and DMI parameters \mathbf{D}_{ij} are calculated from first-principles [see density functional theory (DFT) calculation details in Note I of the Supplemental Material [35]].

\mathbf{D}_{ij} vectors are used to calculate the effective DMI D_{eff} at each monolayer (ML), by analogy with the method in Ref. [12] [inset of Fig. 2(h)]. Although DMI interactions vanish in bulk fcc Co because of symmetry reasons, the impact of the Co/Pt and Co/Ta interfaces on the electronic structure inside the 5-ML Co film is nonvanishing, which leads to finite D_{eff} in all the MLs. This additive interfacial

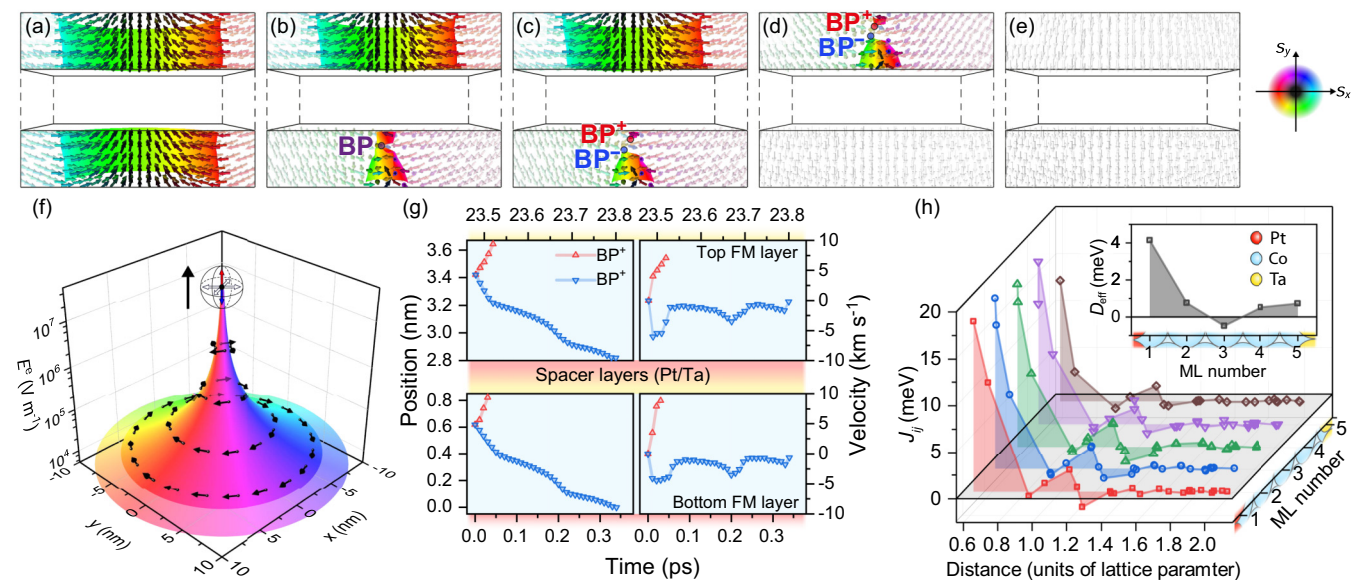


FIG. 2. Bloch-point dynamics and associated emergent electric field during the skyrmion annihilation in a [Pt/Co/Ta]₂ multilayer. (a)–(e) Snapshots of cross-sectional spin profiles in Co layers (Pt and Ta layers are hidden). The color palette represents the spin direction, and isosurfaces indicate the positions of $s_z = 0$. (f) Radiation of emergent electric field \mathbf{E}^e by a moving BP^+ with velocity 2 km s⁻¹. The field has an in-plane vortexlike direction (represented by color and arrows), with the magnitude illustrated in the z dimension. (g) Temporal evolution of the Bloch-point displacement (left-hand side) and velocity (right-hand side) along the out-of-plane direction. The top and bottom FM layers are represented in blue background, separated by Pt (red) and Ta (yellow) NM layers. (h) The pairwise exchange coupling J_{ij} and layer-resolved effective DMI D_{eff} for fcc Co regarding different atomic positions, calculated by the first-principles method.

DMI contributes to the stabilization of Néel-type skyrmions in the multilayer structure [Fig. 2(a)]. Because the continuity of the ferromagnet is broken by nonmagnetic spacers, the spin texture exists in the form of a skyrmion “chain” [Fig. 1(b)], and the components at FM layers are coupled by the magnetostatic interaction [6,7,31]. Notably, additional interactions between adjacent FM layers may also contribute to the skyrmion stabilization in magnetic multilayers, such as the Ruderman-Kittel-Kasuya-Yoshida (RKKY) effect [36,37]. However, regarding the selection of materials in this work, the RKKY coupling of Pt or Ta is sufficiently weak [36], making it reasonable to assume that the interlayer coupling is dominated by the magnetostatic interaction [8]. This stabilization mechanism is different from that of single skyrmion tubes in bulk chiral magnets [9,18] [Fig. 1(a)], where both exchange and magnetostatic couplings coexist throughout the sample. The strength of the long-range magnetostatic coupling is also expected to be smaller than the Heisenberg exchange. Therefore, when being subject to an out-of-plane magnetic field with a critical magnitude, the skyrmion annihilation (see Video 1 in the Supplemental Material [35]) is not initiated simultaneously in all FM layers but starts to unwind from the bottom. During the process, the skyrmion deforms in a radially symmetric manner [38], accompanied by the creation of a pair of Bloch points with each corresponding to a chiral bobber [Fig. 2(b)]. It is worth noting that the Bloch-point pair is created near the middle of a FM layer. It can be explained by the spatially inhomogeneous D_{eff} [inset of Fig. 2(h)], i.e., the DMI near the Pt/Co interface (ML number = 1) holds a much larger magnitude than that near the Co/Ta interface (ML number = 5), which provides more robust stability; moreover, the D_{eff} in the middle of a Co layer (ML number = 3) is the weakest and even has an opposite sign to those near the two interfaces, having a destabilizing effect. After being created, the two Bloch points (BP^+ and BP^-) propagate upward and downward, respectively, until they finally disappear at the FM/NM interfaces [Fig. 2(c)]. Then, affected by the demagnetizing field of the lower FM layer, a new Bloch-point pair is created at the upper FM layer, with the subsequent dynamics following a similar manner [Figs. 2(d) and 2(e)].

The created Bloch points act as magnetic monopoles/antimonopoles, and produce radial emergent magnetic fields $\mathbf{B}^e = g^e \mathbf{r}/r^3$ ($r > 0$) with a quantized emergent charge $g^e = \pm \hbar/2q^e$ ($q^e = \pm 1/2$ for majority/minority electron spins) [39,40]. In the adiabatic limit, for a rigid magnetic Bloch-point texture moving with a drifting velocity \mathbf{v}_{BP} , its magnetization \mathbf{m} can be considered only as a function of time $\mathbf{m}(\mathbf{r}, t) = \mathbf{m}(\mathbf{r} - \mathbf{v}_{\text{BP}}t)$. By analogy with the Faraday’s law of induction by $\mathbf{E}^e = -\mathbf{v}_{\text{BP}} \times \mathbf{B}^e$ [9,20,22], the propagation velocity of a Bloch point (e.g., BP^+) has a magnitude in the order of kilometers per second, and induces an in-plane real electric field in a vortex form perpendicular to the radial direction with a magnitude in the order of megavolts per meter [Fig. 2(f)]. Although these two Bloch points propagate in opposite directions [Fig. 2(g)], their topological charges are also opposite, and as a result, the superimposed electric field radiates in the same direction. It should be emphasized that the propagation is periodically modulated by discrete potential wells between neighboring fcc Co lattice sites [Fig. 2(g)] [9,41] as well as the artificial pinning imposed

by the interlayer spacer (Fig. S1 in the Supplemental Material [35]) which can be experimentally tuned. The velocity magnitude of the Bloch point moving downwards (BP^-) oscillates and reaches another peak at ~ 0.2 ps (~ 23.5 ps) in the bottom (top) FM layer [bottom-right or top-right panel of Fig. 2(g)], with the frequency lying in a terahertz range. Notably, its dynamic behavior and the associated emergent electric field can be manipulated by varying the magnetic parameters [9]. It is fundamentally relevant to the spin-Cherenkov effect [42–44], i.e., the comparison between the phase velocity of the spontaneously emitting spin wave and the propagation velocity of the Bloch point, whose speed limit is dependent on the damping rate.

Interlayer Bloch-point hopping and TH signal. It is known that magnetic skyrmions can provide a quantized topological Hall (TH) response for transport measurements, which is independent of the skyrmion diameter or applied magnetic field [28,29]. It thus points to a superior solution to track the anomalous Hall effect [45] for skyrmion characterization by the unambiguous electrical detection that is linked to potential applications. Previous work [28,29] has shown the intrinsic connection of the TH signal and the number of skyrmions by utilizing their topological nature. However, studies on the emergent TH response properties are necessary when the integrity of the skyrmionic textures is broken [33]. As we have shown, the unwinding of single skyrmions in magnetic multilayers evolves in an inhomogeneous manner as a function of depth. To elucidate the inherent TH signature of such three-dimensional textures, we study the variation of TH resistivity ρ_{xy}^{TH} during the skyrmion annihilation in a $[\text{NM}/\text{FM}/\text{NM}']_{10}$ multilayer. The magnetization dynamics is simulated by a micromagnetic model using MUMAX³ [46] (see results in Note II of the Supplemental Material [35]), as it is more efficient than atomistic models when computing a large-scale system, especially on the calculation of demagnetizing fields. We then numerically verify the transport properties by following a single-orbital tight-binding model [27,28,47] using the KWANT package [48] [schematic of the crossbar setup shown in Fig. 3(a)], where the interaction of electrons with local magnetization fields is described by [27,28,45]

$$H_e = \sum_i c_i^\dagger \epsilon_i c_i - t \sum_{\langle i,j \rangle} (c_i^\dagger c_j + \text{H.c.}) - J_H \sum_i c_i^\dagger \boldsymbol{\sigma}_i \cdot \mathbf{m}_i, \quad (2)$$

where J_H is the Hund’s coupling between the spin $\boldsymbol{\sigma}$ of itinerant electrons and the magnetization \mathbf{m}_i . ϵ_i is the on-site energy of the orbital. t is the hopping integral between nearest-neighbor sites. c_i^\dagger (c_i) is the creation (annihilation) operator of site i . Electronic transmissions are calculated by the Landauer-Büttiker formalism [49] (see method in Note III of the Supplemental Material [35]).

We consider a defect-free system without impurity scatterings, and the on-site energy is neglected. We also assume a strong coupling with $J_H = 5t$ based on the adiabatic approximation [27,50,51], where an electron spin will be constantly adjusted and aligned to the magnetization direction when passing through a magnetic texture. The annihilation process consists of gradually unzipping the skyrmion “chain” from the bottom-most FM layer towards the top (Fig. S1 in

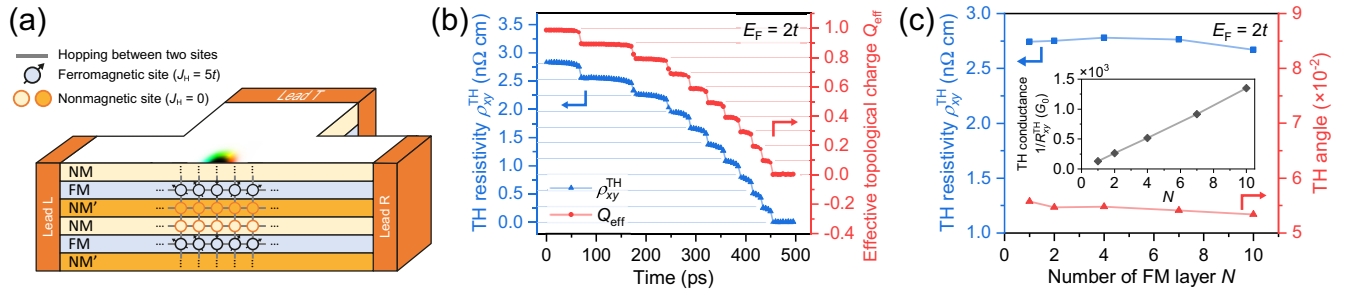


FIG. 3. Topological Hall effect of a multilayer skyrmion. (a) Schematic of a multilayer $[\text{NM}/\text{FM}/\text{NM}']_N$ transport model. The cross section of a four-terminal setup is shown, including a spin texture placed in the center. (b) Temporal evolution of ρ_{xy}^{TH} (blue triangles) and effective topological charge $Q_{\text{eff}} = \frac{1}{N} \sum Q_n$ (red circles) during the annihilation/unwinding process. (c) TH responses including TH resistivity ρ_{xy}^{TH} (blue squares), TH angle θ^{TH} (red triangles), and TH conductance $1/R_{xy}^{\text{TH}}$ (black diamonds in the inset) regarding the total thickness of FM layers (number of FM layers N). Solid lines connecting data points are guides to the eye.

the Supplemental Material [35]). At the beginning, an intact skyrmion chain has the effective topological charge $Q_{\text{eff}} \approx 1$ [Fig. 3(b)]. As it gradually unwinds, breaking into its components, Q_{eff} experiences a stairlike decrease until it reaches “0” when the skyrmion chain is fully unwound to a spin-polarized state. By plotting the temporal evolution of TH resistivity ρ_{xy}^{TH} [Fig. 3(b)], we find that the magnitude is approximately proportional to Q_{eff} .

To further elaborate the intrinsic connection of the TH effect with the effective topological charge of a single skyrmion chain, we focus on the TH response of the magnetic multilayer $[\text{NM}/\text{FM}/\text{NM}']_N$ regarding the total thickness of FM layers (expressed as the number of repeats N). As each component of the chain provides the same amount of channels for electron deflection, the total TH conductance ($1/R_{xy}^{\text{TH}}$) is proportional to N [inset of Fig. 3(c)], whereas both TH resistivity ρ_{xy}^{TH} and TH angle θ^{TH} (V_H/V_x) are independent of N [Fig. 3(c)]. These findings suggest that ρ_{xy}^{TH} can be considered as the “density” of the electron deflection contributed by the N FM layers of the skyrmion chain. Notably, the variation of the transport properties in a bulk chiral system is reported by Redies *et al.* [33], where the Hall conductivity decreases as the heights of the chiral bobbers increase. Furthermore, the associated \mathbf{B}^e of Bloch points will have a pronounced influence on the electronic states. Their demonstration [33] is similar to our findings shown in Fig. 3(b), where a drastic decrease of the TH resistivity ρ_{xy}^{TH} occurs with the presence of Bloch points during the breaking of a skyrmion chain. In previous work [24,25,29,30], ρ_{xy}^{TH} is associated with $\rho_{xy}^{\text{TH}} = PR_0 B_{\text{eff}}^z = PR_0 \phi_0 q_d$ in skyrmionic systems, with the spin polarization P , ordinary Hall coefficient R_0 , and flux quantum ϕ_0 . $q_d = Q/A$ is the density of two-dimensional (2D) topological charge Q within an area A [29,30]. Herein, we extend this equation by considering the overall 3D topology in terms of a nonuniform topological charge density $q_{d,n}$ in the n th FM layer: $\rho_{xy}^{\text{TH}} = \frac{1}{N} PR_0 \phi_0 \sum q_{d,n}$. Conceptually, the variation of ρ_{xy}^{TH} can be attributed to the topological winding/unwinding, which fundamentally manifests the Bloch-point hopping through a distance Δx_{BP} :

$$\Delta \rho_{xy}^{\text{TH}} = PR_0 \phi_0 \frac{\Delta Q}{A} = PR_0 \phi_0 \frac{\Delta x_{\text{BP}}}{V}. \quad (3)$$

Therefore, the dynamics of infinitely small Bloch points within the three-dimensional multilayers’ overall volume V can be indirectly connected. As this phenomenon is also simultaneously accompanied by radiated emergent electric fields \mathbf{E}^e , these results may therefore provide essential ramifications for topological spin textures in nanoscale magnetic multilayers and the link to their electrical detections and potential applications exploiting their associated emergent electromagnetic signatures.

Engineering 3D multistates. To take a step further, we propose a prototype for three-dimensional skyrmionic memory and logic devices by utilizing metastable states of skyrmion chains in magnetic multilayers, which would be relevant to room-temperature multibit technological solutions. Previous work demonstrated various routes of tailoring the magnetic properties (e.g., anisotropy, DMI, and RKKY coupling) by controlling parameters during the thin-film deposition process [37,52,53]. Here, the $[\text{NM}/\text{FM}/\text{NM}']_3$ systems are exemplified, where DMIs are engineered in a layer-dependent manner (Fig. 4). Taking an example of the $\text{DMI} = 2.0/1.8/1.6 \text{ mJ m}^{-2}$ at the top/middle/bottom FM layer [Fig. 4(a₃)], the energy barrier for Bloch-point creations can be sufficiently lowered in a FM layer with smaller DMI. As a result, annihilation processes occur at sufficiently distinct magnetic fields $B_{\text{ext}} = 140/90/50 \text{ mT}$ (see method of “field sweeping” in Note II of the Supplemental Material [35]), and the corresponding TH resistivity ρ_{xy}^{TH} also shows a multilevel feature as a function of the field [green crosses in Fig. 4(b)]. Furthermore, to test the stability of these metastable states [shown in Fig. 4(a₃)] against finite temperature, each state starts from its 0-K equilibrium [in Fig. 4(b)], and a randomly fluctuating thermal field [54] ($T = 300 \text{ K}$) is applied for 20 ns. During the process ρ_{xy}^{TH} is recorded every 0.05 ns for each field and the statistical mean and deviation are calculated. In Fig. 4(c), these states can be well defined, which are approximately proportional to the length of the remnant chain. We should emphasize that the dynamics module in micromagnetics may not precisely emulate the realistic thermal effect for probing the thermostability of spin textures, so future dedicated studies would be needed systematically to evaluate the lifetime of metastable states embedded in magnetic multilayers.

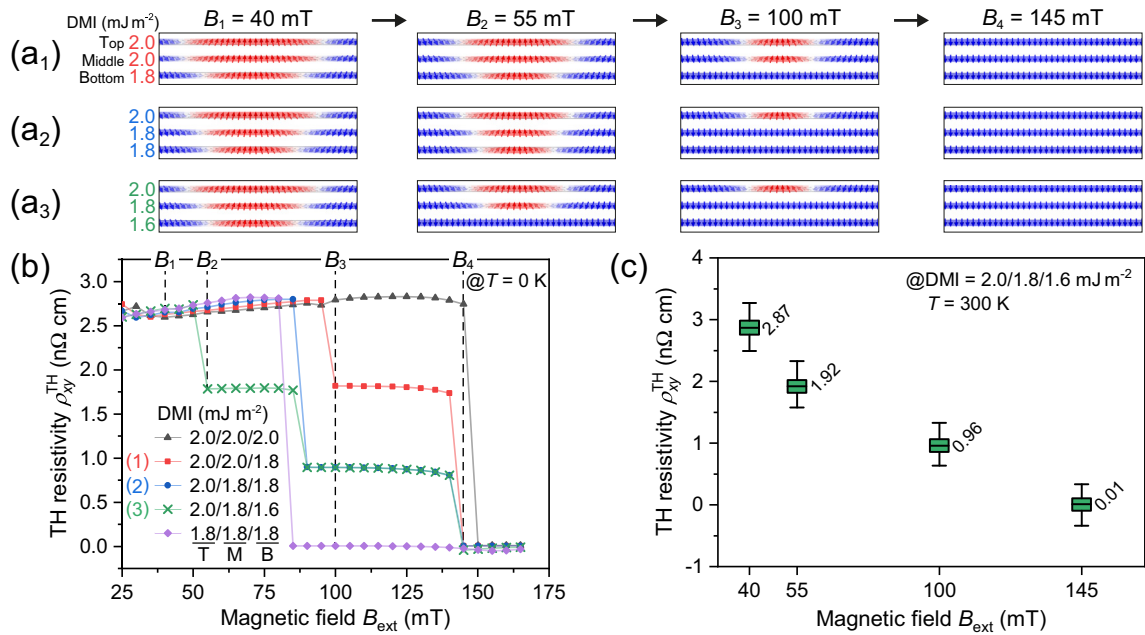


FIG. 4. Multiple metastable states with distinct TH signatures by engineering layer-dependent properties in $[NM/FM/NM']_3$ multilayers. (a) Annihilation processes of a single skyrmion accompanied by multistate behaviors, regarding three cases (a₁)–(a₃) of layer-dependent DMIs. (b) Variation of ρ_{xy}^{TH} as a function of B_{ext} , including the cases corresponding to (a₁) with red squares, (a₂) with blue circles, and (a₃) with green crosses. (c) Statistical means and deviations of ρ_{xy}^{TH} against thermal fluctuations, regarding (a₃) with $DMI = 2.0/1.8/1.6$ mJ m⁻² at the T(top)/M(iddle)/B(ottom) FM layer.

Multilevel bits defined by layer-dependent magnetization states have been demonstrated in various prototypes, including magnetic ratchets [55] and magnetic abacus memories [56]. The device-level performance is expected to be more reliable against external perturbations by utilizing the TH signals, because the topological stability effectively protects the topological charge from continuous variations. Furthermore, in realistic conditions, disordered pinning sites which generally exist in sputtered films may widen the range of critical fields for skyrmion annihilation, or may energetically favor wormlike textures [30]. In such cases the system undergoes gradual metamagnetic transitions which are reflected in a smooth variation of $\rho_{xy}^{TH} - B_{ext}$ loops [30,57,58] rather than the sharp jumps shown in Fig. 4(b). The layer-dependent discontinuities and inhomogeneities of magnetic properties here act as types of “soft pinning” and crucially alter the energy barriers among the metastable states, making it possible to energetically compete against intralayer disorders and even dominate the transition paths.

Conclusions. In this Letter, we have investigated single skyrmions in magnetic multilayers that can exist as skyrmion “chains,” hosted in FM layers and indirectly coupled by magnetostatic interactions. By the application of an external out-of-plane magnetic field, a skyrmion chain starts to unwind from the bottom FM layer, and the process is mediated by the complex dynamics of Bloch points: A pair of Bloch points is created from the weakest-DMI part of an FM layer, and the two Bloch points move towards opposite directions until they finally disappear at the strongest-DMI interfaces. The Bloch-point hopping through layers is modulated by the pinning effect of nonmagnetic spacers, whose thickness can be tuned experimentally. Similar to the mechanism in bulk

chiral magnets [9], the Bloch-point propagation gives rise to a vortexlike emergent electric field perpendicular to the propagation direction, with MV/m magnitude and THz oscillation frequency. On the other hand, its displacement induces a variation in the TH response, and the resistivity experiences a stairlike decrease with the magnitude approximately proportional to the effective topological charge. Furthermore, we propose that metastable states in the skyrmion chain can be thermodynamically stabilized by tailoring the layer-dependent properties of materials, by means of, for example, engineering different DMI in the layers. These states have distinct TH signatures, and can be switched by simply varying the external magnetic field. Our findings elucidate magnetic-multilayer skyrmions and their three-dimensional topology that could significantly enrich the availability of transport signatures in multilayer nontrivial spin textures. In addition, this work proposes a paradigm of three-dimensional devices embedded with multibit functionalities. By building on recent proposals in three-dimensional spintronics [55,56,59], our results point to fruitful directions of practical room-temperature applications, in technologically relevant multilayers where experimental evidence is within reach.

Acknowledgments. Financial support by the EP/V028189/1 grant and by the DFG via SFB 1277 (Emergente Relativistische Effekte in der Kondensierten Materie) is gratefully acknowledged. The authors would like to acknowledge the assistance given by Research IT and the use of the Computational Shared Facility at The University of Manchester. Y.L. acknowledges the funding support by the University of Manchester and the China Scholarship Council.

- [1] A. Fert, N. Reyren, and V. Cros, Magnetic skyrmions: Advances in physics and potential applications, *Nat. Rev. Mater.* **2**, 17031 (2017).
- [2] N. Nagaosa, Emergent electromagnetism in condensed matter, *Proc. Jpn. Acad. Ser. B* **95**, 278 (2019).
- [3] C. Back, V. Cros, H. Ebert, K. Everschor-Sitte, A. Fert, M. Garst, T. Ma, S. Mankovsky, T. L. Monchesky, M. Mostovoy, N. Nagaosa, S. S. P. Parkin, C. Pfleiderer, N. Reyren, A. Rosch, Y. Taguchi, Y. Tokura, K. von Bergmann, and J. Zang, The 2020 Skyrmionics Roadmap, *J. Phys. D: Appl. Phys.* **53**, 363001 (2020).
- [4] I. Dzyaloshinsky, A thermodynamic theory of weak ferromagnetism of antiferromagnetics, *J. Phys. Chem. Solids* **4**, 241 (1958).
- [5] T. Moriya, Anisotropic Superexchange Interaction and Weak Ferromagnetism, *Phys. Rev.* **120**, 91 (1960).
- [6] W. Legrand, N. Ronceray, N. Reyren, D. Maccariello, V. Cros, and A. Fert, Modeling the Shape of Axisymmetric Skyrmions in Magnetic Multilayers, *Phys. Rev. Applied* **10**, 064042 (2018).
- [7] I. Lemesh and G. S. D. Beach, Walker Breakdown with a Twist: Dynamics of Multilayer Domain Walls and Skyrmions Driven by Spin-Orbit Torque, *Phys. Rev. Appl.* **12**, 044031 (2019).
- [8] J. Lucassen, M. J. Meijer, O. Kurnosikov, H. J. M. Swagten, B. Koopmans, R. Lavrijsen, F. Klodt-Twesten, R. Frömter, and R. A. Duine, Tuning Magnetic Chirality by Dipolar Interactions, *Phys. Rev. Lett.* **123**, 157201 (2019).
- [9] Y. Li, L. Pierobon, M. Charilaou, H.-B. Braun, N. R. Walet, J. F. Löffler, J. J. Miles, and C. Moutafis, Tunable terahertz oscillation arising from Bloch-point dynamics in chiral magnets, *Phys. Rev. Research* **2**, 033006 (2020).
- [10] H.-B. Braun, Topological effects in nanomagnetism: From superparamagnetism to chiral quantum solitons, *Adv. Phys.* **61**, 1 (2012).
- [11] A. Fert and P. M. Levy, Role of Anisotropic Exchange Interactions in Determining the Properties of Spin-Glasses, *Phys. Rev. Lett.* **44**, 1538 (1980).
- [12] H. Yang, A. Thiaville, S. Rohart, A. Fert, and M. Chshiev, Anatomy of Dzyaloshinskii-Moriya Interaction at Co/Pt Interfaces, *Phys. Rev. Lett.* **115**, 267210 (2015).
- [13] C. Moreau-Luchaire, C. Moutafis, N. Reyren, J. Sampaio, C. A. F. Vaz, N. Van Horne, K. Bouzehouane, K. Garcia, C. Deranlot, P. Warnicke, P. Wohlhüter, J.-M. George, M. Weigand, J. Raabe, V. Cros, and A. Fert, Additive interfacial chiral interaction in multilayers for stabilization of small individual skyrmions at room temperature, *Nat. Nanotechnol.* **11**, 444 (2016).
- [14] O. Boulle, J. Vogel, H. Yang, S. Pizzini, D. d. S. Chaves, A. Locatelli, T. O. Mentş, A. Sala, L. D. Buda-Prejbeanu, O. Klein, M. Belmeguenai, Y. Roussigné, A. Stashkevich, S. M. Chéri, I. M. Miron, and G. Gaudin, Room-temperature chiral magnetic skyrmions in ultrathin magnetic nanostructures, *Nat. Nanotechnol.* **11**, 449 (2016).
- [15] S. Woo, K. Litzius, B. Krüger, M. Y. Im, L. Caretta, K. Richter, M. Mann, A. Krone, R. M. Reeve, M. Weigand, P. Agrawal, I. Lemesh, M. A. Mawass, P. Fischer, M. Kläui, and G. S. D. Beach, Observation of room-temperature magnetic skyrmions and their current-driven dynamics in ultrathin metallic ferromagnets, *Nat. Mater.* **15**, 501 (2016).
- [16] A. P. Malozemoff and J. C. Slonczewski, *Magnetic Domain Walls in Bubble Materials: Advances in Materials and Device Research* (Academic, New York, 1979).
- [17] M. T. Birch, D. Cortés-Ortuño, L. A. Turnbull, M. N. Wilson, F. Groß, N. Träger, A. Laurensen, N. Bukin, S. H. Moody, M. Weigand, G. Schütz, H. Popescu, R. Fan, P. Steadman, J. A. Verezhak, G. Balakrishnan, J. C. Loudon, A. C. Twitchett-Harrison, O. Hovorka, H. Fangohr, F. Y. Ogrin, J. Gräfe, and P. D. Hatton, Real-space imaging of confined magnetic skyrmion tubes, *Nat. Commun.* **11**, 1726 (2020).
- [18] P. Milde, D. Köhler, J. Seidel, L. M. Eng, A. Bauer, A. Chacon, J. Kindervater, S. Mühlbauer, C. Pfleiderer, S. Buhdrandt, C. Schütte, and A. Rosch, Unwinding of a skyrmion lattice by magnetic monopoles, *Science* **340**, 1076 (2013).
- [19] P. Wohlhüter, M. T. Bryan, P. Warnicke, S. Gliga, S. E. Stevenson, G. Heldt, L. Saharan, A. K. Suszka, C. Moutafis, R. V. Chopdekar, J. Raabe, T. Thomson, G. Hrkac, and L. J. Heyderman, Nanoscale switch for vortex polarization mediated by Bloch core formation in magnetic hybrid systems, *Nat. Commun.* **6**, 7836 (2015).
- [20] T. Schulz, R. Ritz, A. Bauer, M. Halder, M. Wagner, C. Franz, C. Pfleiderer, K. Everschor, M. Garst, and A. Rosch, Emergent electrostatics of skyrmions in a chiral magnet, *Nat. Phys.* **8**, 301 (2012).
- [21] K. Everschor-Sitte and M. Sitte, Real-space Berry phases: Skyrmion soccer (invited), *J. Appl. Phys.* **115**, 172602 (2014).
- [22] M. Charilaou, H.-B. Braun, and J. F. Löffler, Monopole-Induced Emergent Electric Fields in Ferromagnetic Nanowires, *Phys. Rev. Lett.* **121**, 097202 (2018).
- [23] J. Ye, Y. B. Kim, A. J. Millis, B. I. Shraiman, P. Majumdar, and Z. Tešanović, Berry Phase Theory of the Anomalous Hall Effect: Application to Colossal Magnetoresistance Manganites, *Phys. Rev. Lett.* **83**, 3737 (1999).
- [24] G. Tatara, H. Kohno, J. Shibata, Y. Lemaho, and K.-J. Lee, Spin torque and force due to current for general spin textures, *J. Phys. Soc. Jpn.* **76**, 054707 (2007).
- [25] A. Neubauer, C. Pfleiderer, B. Binz, A. Rosch, R. Ritz, P. G. Niklowitz, and P. Böni, Topological Hall Effect in the A Phase of MnSi, *Phys. Rev. Lett.* **102**, 186602 (2009).
- [26] C. Franz, F. Freimuth, A. Bauer, R. Ritz, C. Schnarr, C. Duvinage, T. Adams, S. Blügel, A. Rosch, Y. Mokrousov, and C. Pfleiderer, Real-Space and Reciprocal-Space Berry Phases in the Hall Effect of Mn_{1-x}Fe_xSi, *Phys. Rev. Lett.* **112**, 186601 (2014).
- [27] G. Yin, Y. Liu, Y. Barlas, J. Zang, and R. K. Lake, Topological spin Hall effect resulting from magnetic skyrmions, *Phys. Rev. B* **92**, 024411 (2015).
- [28] P. B. Ndiaye, C. A. Akosa, and A. Manchon, Topological Hall and spin Hall effects in disordered skyrmionic textures, *Phys. Rev. B* **95**, 064426 (2017).
- [29] K. Zeissler, S. Finizio, K. Shahbazi, J. Massey, F. A. Ma’Mari, D. M. Bracher, A. Kleibert, M. C. Rosamond, E. H. Linfield, T. A. Moore, J. Raabe, G. Burnell, and C. H. Marrows, Discrete Hall resistivity contribution from Néel skyrmions in multilayer nanodiscs, *Nat. Nanotechnol.* **13**, 1161 (2018).
- [30] M. Raju, A. Yagil, A. Soumyanarayanan, A. K. Tan, A. Almoalem, F. Ma, O. M. Auslaender, and C. Panagopoulos, The evolution of skyrmions in Ir/Fe/Co/Pt multilayers and their topological Hall signature, *Nat. Commun.* **10**, 696 (2019).

- [31] W. Legrand, J.-Y. Chauleau, D. Maccariello, N. Reyren, S. Collin, K. Bouzehouane, N. Jaouen, V. Cros, and A. Fert, Hybrid chiral domain walls and skyrmions in magnetic multilayers, *Sci. Adv.* **4**, eaat0415 (2018).
- [32] D. M. Burn, S. L. Zhang, G. Q. Yu, Y. Guang, H. J. Chen, X. P. Qiu, G. van der Laan, and T. Hesjedal, Depth-Resolved Magnetization Dynamics Revealed by X-Ray Reflectometry Ferromagnetic Resonance, *Phys. Rev. Lett.* **125**, 137201 (2020).
- [33] M. Redies, F. R. Lux, J.-P. Hanke, P. M. Buhl, G. P. Müller, N. S. Kiselev, S. Blügel, and Y. Mokrousov, Distinct magneto-transport and orbital fingerprints of chiral bobbers, *Phys. Rev. B* **99**, 140407(R) (2019).
- [34] G. P. Müller, M. Hoffmann, C. Dißelkamp, D. Schürhoff, S. Mavros, M. Sallermann, N. S. Kiselev, H. Jónsson, and S. Blügel, Spirit: Multifunctional framework for atomistic spin simulations, *Phys. Rev. B* **99**, 224414 (2019).
- [35] See Supplemental Material at <http://link.aps.org/supplemental/10.1103/PhysRevB.104.L140409> for (I) details and some results of DFT calculations, (II) micromagnetic results of the annihilation of a single multilayer skyrmion, and (III) the method of the Landauer-Büttiker formalism for charge currents, which includes Refs. [60–68].
- [36] S. S. P. Parkin, Systematic Variation of the Strength and Oscillation Period of Indirect Magnetic Exchange Coupling through the $3d$, $4d$, and $5d$ Transition Metals, *Phys. Rev. Lett.* **67**, 3598 (1991).
- [37] W. Legrand, D. Maccariello, F. Ajejas, S. Collin, A. Vecchiola, K. Bouzehouane, N. Reyren, V. Cros, and A. Fert, Room-temperature stabilization of antiferromagnetic skyrmions in synthetic antiferromagnets, *Nat. Mater.* **19**, 34 (2020).
- [38] F. Muckel, S. von Malotki, C. Holl, B. Pestka, M. Prutzer, P. F. Bessarab, S. Heinze, and M. Morgenstern, Experimental identification of two distinct skyrmion collapse mechanisms, *Nat. Phys.* **17**, 395 (2021).
- [39] D. J. Griffiths, *Introduction to Electrodynamics*, 4th ed. (Cambridge University Press, Cambridge, UK, 2017).
- [40] *Topological Structures in Ferroic Materials*, edited by J. Seidel (Springer, Berlin, 2016).
- [41] S. K. Kim and O. Tchernyshyov, Pinning of a Bloch point by an atomic lattice, *Phys. Rev. B* **88**, 174402 (2013).
- [42] D. Bouzidi and H. Suhl, Motion of a Bloch Domain Wall, *Phys. Rev. Lett.* **65**, 2587 (1990).
- [43] R. Hertel, Ultrafast domain wall dynamics in magnetic nanotubes and nanowires, *J. Phys.: Condens. Matter* **28**, 483002 (2016).
- [44] X.-P. Ma, J. Zheng, H.-G. Piao, D.-H. Kim, and P. Fischer, Cherenkov-type three-dimensional breakdown behavior of the Bloch-point domain wall motion in the cylindrical nanowire, *Appl. Phys. Lett.* **117**, 062402 (2020).
- [45] N. Nagaosa, J. Sinova, S. Onoda, A. H. MacDonald, and N. P. Ong, Anomalous Hall effect, *Rev. Mod. Phys.* **82**, 1539 (2010).
- [46] A. Vansteenkiste, J. Leliaert, M. Dvornik, M. Helsen, F. Garcia-Sanchez, and B. V. Waeyenberge, The design and verification of MuMax3, *AIP Adv.* **4**, 107133 (2014).
- [47] B. Göbel, A. F. Schäffer, J. Berakdar, I. Mertig, and S. S. P. Parkin, Electrical writing, deleting, reading, and moving of magnetic skyrmioniums in a racetrack device, *Sci. Rep.* **9**, 12119 (2019).
- [48] C. W. Groth, M. Wimmer, A. R. Akhmerov, and X. Waintal, Kwant: A software package for quantum transport, *New J. Phys.* **16**, 063065 (2014).
- [49] S. Datta, *Electronic Transport in Mesoscopic Systems*, Cambridge Studies in Semiconductor Physics and Microelectronic Engineering (Cambridge University Press, Cambridge, UK, 1995).
- [50] K. S. Denisov, I. V. Rozhansky, N. S. Averkiev, and E. Lähderanta, General theory of the topological Hall effect in systems with chiral spin textures, *Phys. Rev. B* **98**, 195439 (2018).
- [51] K. Nakazawa and H. Kohno, Weak coupling theory of topological Hall effect, *Phys. Rev. B* **99**, 174425 (2019).
- [52] M. S. Gabor, T. Petrisor, R. B. Mos, M. Nasui, C. Tiusan, and T. Petrisor, Interlayer exchange coupling in perpendicularly magnetized Pt/Co/Ir/Co/Pt structures, *J. Phys. D: Appl. Phys.* **50**, 465004 (2017).
- [53] D. Khadka, S. Karayev, and S. X. Huang, Dzyaloshinskii-Moriya interaction in Pt/Co/Ir and Pt/Co/Ru multilayer films, *J. Appl. Phys.* **123**, 123905 (2018).
- [54] W. F. Brown, Thermal fluctuations of a single-domain particle, *Phys. Rev.* **130**, 1677 (1963).
- [55] R. Lavrijsen, J.-H. Lee, A. Fernández-Pacheco, D. C. M. C. Petit, R. Mansell, and R. P. Cowburn, Magnetic ratchet for three-dimensional spintronic memory and logic, *Nature (London)* **493**, 647 (2013).
- [56] S. Zhang, J. Zhang, A. A. Baker, S. Wang, G. Yu, and T. Hesjedal, Three dimensional magnetic abacus memory, *Sci. Rep.* **4**, 6109 (2014).
- [57] L. Pierobon, C. Moutafis, Y. Li, J. F. Löffler, and M. Charilaou, Collective antiskyrmion-mediated phase transition and defect-induced melting in chiral magnetic films, *Sci. Rep.* **8**, 16675 (2018).
- [58] A. Soumyanarayanan, M. Raju, A. L. Gonzalez Oyarce, A. K. C. Tan, M.-Y. Im, A. P. Petrović, P. Ho, K. H. Khoo, M. Tran, C. K. Gan, F. Ernult, and C. Panagopoulos, Tunable room-temperature magnetic skyrmions in Ir/Fe/Co/Pt multilayers, *Nat. Mater.* **16**, 898 (2017).
- [59] A. Fernández-Pacheco, R. Streubel, O. Fruchart, R. Hertel, P. Fischer, and R. P. Cowburn, Three-dimensional nanomagnetism, *Nat. Commun.* **8**, 15756 (2017).
- [60] H. Ebert and S. Mankovsky, Anisotropic exchange coupling in diluted magnetic semiconductors: *Ab initio* spin-density functional theory, *Phys. Rev. B* **79**, 045209 (2009).
- [61] S. Mankovsky and H. Ebert, Accurate scheme to calculate the interatomic Dzyaloshinskii-Moriya interaction parameters, *Phys. Rev. B* **96**, 104416 (2017).
- [62] H. Ebert, D. Ködderitzsch, and J. Minár, Calculating condensed matter properties using the KKR-green's function method—recent developments and applications, *Rep. Prog. Phys.* **74**, 096501 (2011).
- [63] H. Ebert *et al.*, The Munich SPR-KKR package, version 7.7, <https://www.ebert.cup.uni-muenchen.de/en/software-en/13-sprkkp>.
- [64] S. H. Vosko, L. Wilk, and M. Nusair, Accurate spin-dependent electron liquid correlation energies for local spin density calculations: A critical analysis, *Can. J. Phys.* **58**, 1200 (1980).

- [65] Q. Bai, J. Mao, J. Yun, Y. Zhai, M. Chang, X. Zhang, J. Zhang, Y. Zuo, and L. Xi, In-plane crystallographic orientations related spin-orbit torque in epitaxial Pt(111)/Co/Ta heterostructures, *Appl. Phys. Lett.* **118**, 132403 (2021).
- [66] G. Kresse and J. Hafner, *Ab initio* molecular dynamics for liquid metals, *Phys. Rev. B* **47**, 558 (1993).
- [67] G. Kresse and J. Hafner, Norm-conserving and ultrasoft pseudopotentials for first-row and transition elements, *J. Phys.: Condens. Matter* **6**, 8245 (1994).
- [68] J. P. Perdew, K. Burke, and M. Ernzerhof, Generalized Gradient Approximation Made Simple, *Phys. Rev. Lett.* **77**, 3865 (1996).

Correction: A minor error in a term in Eq. (2) has been fixed.